Journal of Membrane Science 690 (2024) 122202

Contents lists available at ScienceDirect

Journal of Membrane Science

journal homepage: www.elsevier.com/locate/memsci

Analyzing ion uptake in ion-exchange membranes using ion association model

Yaeli S. Oren [a], Oded Nir [a], Viatcheslav Freger [b,c,d,*]

[a] Department of Desalination and Water Treatment, Zuckerberg Institute for Water Research, The Jacob Blaustein Institutes for Desert Research, Ben-Gurion University of the Negev, Sede-Boqer Campus, 8499000, Israel
[b] Wolfson Department of Chemical Engineering, Technion – IIT, Haifa, 32000, Israel
[c] Nancy and Stephen Grand Technion Energy Program, Technion - IIT, Haifa, Israel
[d] Grand Water Research Institute, Technion - IIT, Haifa, Israel

ARTICLE INFO

Keywords:
Membrane transport theory
Ion association and pairing
Ion exchange membranes
Ion partitioning
Ion permeability
Manning condensation

ABSTRACT

Predicting ion uptake and selectivity in ion-exchange membranes is desired for many applications, yet a suitable physical description defining the most appropriate ion-specific parameters is still challenging. Here, we systematically develop an ion-association-based approach to modeling ion uptake in ion-exchange membranes from solutions of symmetric and non-symmetric salts. The model treats association in an ion-specific manner, self-consistently accounting for equilibria between free ions in solution and within the membrane phase (salt injection) and between free and associated species within the membrane (association equilibria), subjects to overall membrane electroneutrality. The resulting models, including different possible association equilibria, were employed to fit the reported data for Nafion 117 and CR61 cation-exchange membranes in equilibrium with NaCl, $MgCl_2$, $CaCl_2$, and Na_2SO_4 single-salt solutions. The results are compared with the previously reported fits to the Manning condensation model, which shows that both models produce similarly good fits for NaCl, $MgCl_2$, and $CaCl_2$ solutions in the 0.01 to 1 M range. However, the greater flexibility and specificity of the association model allow addressing deviations observed for Na_2SO_4 solutions and for $CaCl_2$ above 1 M as free-ion paring and possible formation of charged $NaSO_4^-$ and $CaCl^+$ pairs, respectively. The results demonstrate the present model may be a sound non-mean-field alternative to the Manning condensation model, capable of addressing ion-specificity and multiple modes of association.

1. Introduction

Ion exchange membranes (IEMs) are key enabling components in many important applications [1], including rapidly expanding fields of electrolysis and fuel cells, as well as acid recovery and production, base redox flow batteries, and direct and reverse electrodialysis (ED) [2–5]. The range of IEMs extends from classical homogeneous cation exchange (CEMs) and anion exchange membranes (AEMs) to more sophisticated emerging materials such as multilayer mono/divalent permselective multilayers [6,7], bipolar membranes [8], polyelectrolyte complexes [9], and mixed matrix membranes [10,11]. Despite the fact that IEMs have been successfully used for decades and provide the platform for many recent technological advances, there are still significant gaps in understanding and modeling the underlying thermodynamics, transport, and selectivity towards specific ions, which hinders the development of next-generation IEM materials [12,13]. This lack of fundamental understanding has implications for modeling other membrane processes as well, such as pressure-driven membrane desalination, targeting total or selective ion rejection.

Classical thermodynamic modeling of ion uptake, which is central in ion transport modeling, usually treats the membrane as a homogeneous medium with fixed-charged groups. In some cases, IEMs can be microphase-separated and thus contain phases, within ions present mainly in the water-rich microphase. A uniform Donnan potential is imposed within the membrane or water-rich microphase on all ionic species, which are assumed to behave as free dissociated ions [14–16]. However, as discussed by Kamcev et al. recently, this picture still shows many inconsistencies, and a comprehensive understanding of ion thermodynamics and transport in charged membranes at the molecular level is still missing. The fundamentally sound models that can analyze and fit

* Corresponding author. Wolfson Department of Chemical Engineering, Technion – IIT, Haifa, 32000, Israel.
E-mail address: vfreger@technion.ac.il (V. Freger).

https://doi.org/10.1016/j.memsci.2023.122202
Received 26 July 2023; Received in revised form 14 October 2023; Accepted 22 October 2023
Available online 24 October 2023

and, ultimately, predict permselectivity based on physicochemical membrane characteristics (chemical structure of membrane phases, water content, fixed charge content, etc.) remain a challenge at present [17] and are in the focus of the present study.

Kitto and Kamcev comprehensively reviewed the current state of understanding ion equilibria and transport in ion exchange materials [18]. Specifically, regarding thermodynamic modeling, they reviewed major recent advances beyond the classical Donnan model. The most actively pursued approach in the past decade has been the one based on Manning's counterion condensation theory. For several thoroughly studied materials, these state-of-the-art models showed a good correlation with Manning's limiting law. However, Yu et al. pointed to deviations from Manning's limiting law at concentrations lower than 0.1 M [19]. These authors further proposed a polyelectrolyte non-random two-liquid (pent) model that was applied to data obtained from Yan et al. [20] for a series of AMPS-PEGDA cation exchange membranes of varied ion exchange capacity. The peNRTL model combines Manning's limiting law with the electrolyte non-random two-liquid model, which considers an unsymmetric scaling of ion activity coefficient and relies on knowledge of the (dimensionless) polymer charge density and interaction parameters, which are obtained from regression analysis of experimental data on single-salt partitioning.

As emphasized recently [21], in contrast to aqueous solutions, most membrane materials, including desalination membranes and a majority of IEMs, fall into the category of low-dielectric or low-T* materials, in which the range of electrostatic interactions, defined by the Bjerrum length λ_B, is commensurate or exceeds the inter-ionic distances. As a result, strong electrostatic ion-ion interactions, including those with fixed charges, promote ion association or pairing in the manner first considered by Bjerrum. As such, it is no longer amenable to mean-field description, i.e., in terms of mean potential fields such as a Donnan potential. The same issues arise in narrow nanochannels surrounded by low dielectric matrices [22,23]. In this respect, Manning's condensation model does include association, yet as a special case of the mean-field treatment for a rod-like polymer geometry above a critical fixed charge density in the manner of a phase transition. Thus, it lacks ion specificity, unlike Bjerrum's model, which is not mean-field and ion-specific and predicts a gradual change in the degree of association with fixed charge density and mobile ion concentration, analogous to the behavior of weak electrolytes in solutions.

The main purpose of the present study is to systematically develop the association model of the Bjerrum type outlined previously [21] and critically compare it with the Manning-type model using reported data. To this end, we employ experimental data and modeling results by Sujanani et al. for NaCl, $MgCl_2$, and Na_2SO_4 salt uptake in Nafion 117 membrane [24] and by Galizia et al. for $CaCl_2$ in a CR61 membrane [25]. Compelling evidence of a strong association in Nafion in equilibrium with HCl of different concentrations was reported by Balsara [26]. Münchinger and Kreuer [27] explicitly demonstrated ion specificity of association in co-ion-free Li^+ and Cs^+ forms of Nafion and pointed out the lack of specificity within Manning's picture. Here, these arguments will be systematically developed into quantitative relations, considering the formation of appropriate associated species and their effect on observed counter- and co-ion uptake at different salt concentrations.

2. Model

As an approximation, the membrane is divided to unit cells, each containing a fixed charge group, viewed as a binding site. The volume of a unit cell is then $L^3 = (XN_A)^{-1}$, where N_A is the Avogadro number and X is the nominal fixed charge density (ion exchange capacity) of the membrane or in the aqueous microphase in the case of a microphase-separated membrane in units of mol/m^3. Following the general argument put forward previously and applicable to low-T^* membranes [21], we consider the one-site grand partition function Ξ that sums up statistically the dissociated and appropriate associated states of a fixed charge or, equivalently, a unit cell of the membrane, as follows

$$\Xi = 1 + K_{XM}[M^+] + K_{XM_2}[M^+]^2 + K_{XMA}[M^+][A^-] + \ldots \quad (1)$$

Here, the first term represents the dissociated state of the fixed charges X^-, the second term the state when it forms a pair with one counter-ion M^+, the third when it forms a triplet with two counter-ions, the fourth when it forms a triplet with one counter-ion M^+ and one co-ion A^- etc., where K's are the corresponding association constants and square brackets designate concentration of corresponding free (i.e., dissociated) ion species *in the membrane*. The physical meaning of all K's is the difference in the excess free energy of the corresponding state relative to the dissociated state X^-, therefore the weighing factor for the dissociated state, represented by the first term, is 1. Eq. (1) with just the first two terms is fully analogous to the Langmuir isotherm that assumes only two possible states, free and occupied, which is generalized here it to a larger number of possible states.

The average fraction of each state *in the total fixed charge* is the ratio of the corresponding term in Eq. (1) to the entire Ξ. For instance, the fraction of dissociated fixed charges is $[X^-]/X = 1/\Xi$, the fraction of fixed charges forming MX pairs is $[MX]/X = K_{MX}[M^+]/\Xi$ etc. Free mobile ions M^+ and A^-, not forming pairs, triplets etc. with the fixed charges, are assumed to be present in the membrane *in addition* to the associated states and distributed uniformly over the entire membrane, i.e., equally likely in each unit cell. This is a gross approximation, as explained next, and its validity and applicability will be discussed later on.

It is expedient to define the Bjerrum length λ_B, as follows

$$\lambda_B = \frac{z_i z_j e^2}{4\pi\varepsilon_0\varepsilon_r r_i k_B T} \quad (2)$$

where r_i is the ion radius, ε_r is the dielectric constant of the membrane phase, k_B is the Boltzmann constant, T is the temperature, z is the valency of the ions, and e is the elemental charge. Within the Bjerrum theory of association, $\lambda_B/2$ is the distance to counter-ion within which they are effectively associated. Since, the first counter-ion in a cell is within the distance $L/2$ from the fixed charge, it may not be considered free when λ_B exceeds L, average spacing of fixed charges or, roughly, unit cell diameter. Furthermore, this will also be true for any subsequent ion when the fixed charge binds a counter-ion of M^{2+} type, forming a charged pair MX^+. Yet, when the MX pair is neutral, as for MA or M_2A salts, the pair aligned to maximize its interaction with the subsequent ion will form a triplet within a distance shorter by a factor $\sim 2(b/\lambda_B)^{1/2}$, where $b \approx 2r_i$ is the ion-ion distance in the pair [21]. For the examples of Nafion below, average λ_B was estimated to be 2.8 nm and b is typically 0.3-0.4 nm, the association range of triplets such as M_2X^+ and MAX^- is about half the association range of a MX^0 pair. On the other hand, in the examples below, the unit cell size L is of the order 1.5 nm, which would still leave no or a small fraction of the total membrane volume where ions may considered as free. For divalent ions, it becomes even less likely, as the corresponding association ranges are twice longer.

However, the above estimate of λ_B represents the macroscopic average of the entire membrane, while local values in the aqueous microphase, where the ions are present and interact, may be significantly smaller. While the local value of λ_B is difficult to estimate, we presume this may be small enough to have room for the free mobile ions, M^+ or M^{2+} and A^- or A^{2-}, and it is not unreasonable to simplify the model and "smear" their concentration [M] and [A] uniformly over the entire membrane volume. Yet, these free ions, not included in association equilibria, may still non-negligibly interact with the dissociated fixed charge, pairs, triplets etc. This will affect the relation between the activities and concentrations of free mobile ions within the membrane hence their relation to salt concentration in solution, as expressed by the salt injection coefficient S_0 defined and used below. The parameter S_0 is then interpreted as not coming just from solvation or dielectric exclusion, as in its original definition [21], but also lumping in the mean-field

manner the ion-ion, ion-pair etc. interactions not included in the association equilibria.

The concentrations [M] and [A] represent the actual average *concentrations* of these ions, not found in the assumed associated states. However, in the association terms in Eq. (1), strictly speaking, they must be understood as *activities* within the membrane phase. That means that the association constants K defined in Eq. (1) also include factors related to ion-ion interactions, similar to those lumped to S_0 but not necessarily identical, since relevant (non-uniform) ion-ion potentials average differently in K and S_0. Ultimately, the concentrations [M] and [A] in the membrane are dictated by (i) equilibrium with the salt solution, through S_0, (ii) equilibrium with the associated species within the membrane i.e., each unit cell, through appropriate association constants K, and subject to (iii) the overall electroneutrality of the membrane phase. Below, we derive ion uptake relations for different types of salts satisfying all three conditions.

2.1. MA salts

For MA salts (monovalent cation and anion, such as NaCl), we consider the MX pairs formed by the membrane's charged groups X^- and cations M^+ to be the only associated species. We then neglect associates of third and higher orders, such as MAX, as well as MA pairs of free ions. As explained in Ref. [21], the reason is that their concentrations are determined by higher-order products of free-ion concentrations, which makes them small. For instance, both [MAX] and [MA] will be proportional to the product $[M^+][A^-]$ that is, in turn, proportional to salt concentration in solution *squared* and should be small, see Eq. (5) below. Then Eq. (1) reduces to

$$\Xi = 1 + K_{MX}[M^+], \tag{3}$$

where K_{MX} is the association constant of the MX pair. Since the free fixed charges have a charge -1 while their average number per fixed charge is $1/\Xi$, and since the MX pair is not charged, the average residual charge per fixed charge is $(-1) \times 1/\Xi$. The membrane electroneutrality is then obtained by adding it to the charge of free mobile ions contained in the unit volume $1/X$ and requiring the sum be equal to zero, as follows

$$\frac{-1}{1 + K_{MX}[M^+]} + \frac{[M^+] - [A^-]}{X} = 0. \tag{4}$$

Finally, the free anion and cation concentration in the membrane, $[A^-]$ and $[M^+]$, must satisfy equilibrium with bulk solution, which for MA salts is expressed as [21].

$$[A^-] = \frac{(S_0 C_s)^2}{[M^+]} \tag{5}$$

where S_0 is the dimensionless salt injection coefficient that expresses the overall affinity of the salt to the membrane, the geometric mean of cation, and anion affinities (aka non-Donnan partitioning coefficients), and C_s is the molar salt concentration in solution. The affinities were originally defined to account for the solvation (dielectric) and steric exclusion [21,28], but here they may also contain ion-ion interactions not included in the association equilibria, as explained above. Note that the specific form of Eq. (5) and analogous relations below avoid any explicit consideration of inter-phase (Donnan) potential difference, since it cancels out in the $[M^+][A^-]$ product or analogous products for other salts presented below.

After substituting Eq. (5) to Eq. (4) and solving for $[M^+]$, the average total number of M^+ and A^- ions per unit cell (or fixed charge) as a function of C_s is obtained as

$$\overline{n}_M = \frac{K_{MX}[M^+]}{1 + K_{MX}[M^+]} + \frac{[M^+]}{X} \tag{6}$$

and

$$\overline{n}_A = \frac{[A^-]}{X} = \frac{(S_0 C_s)^2}{X[M^+]}, \tag{7}$$

where the first term in Eq. (6), reminiscent of the Langmuir isotherm, corresponds to associated M^+ ions, and the other term in Eq. (6) and Eq. (7) correspond to free mobile ions. The total concentration of each ion in the membrane, the sum of free and associated, is found by multiplying the average number of ions per fixed charge, $\overline{n}_M$ or $\overline{n}_A$, with the total fixed charge density, X. This yields the following relations that may be directly compared with the measured content of co- and counterions in the membrane

$$C_M^m = X + C_A^m = X + \frac{(S_0 C_S)^2}{[M^+]}; \quad C_A^m = X\overline{n}_A = \frac{(S_0 C_S)^2}{[M^+]}. \tag{8}$$

2.2. MA_2 salts

For MA_2 salts of a divalent cation and monovalent anion, such as $CaCl_2$, the derivation follows the same line as for MA salts. Again, we first assume pairing of the fixed charges with the cations only, but since, in this case, the cation is divalent, the pair is charged, MX^+, and contributes a unit positive charge, turning the electroneutrality to

$$\frac{-1 + K_{MX}[M^{2+}]}{\Xi} + \frac{2[M^{2+}] - [A^-]}{X} = 0, \tag{9}$$

where now $\Xi = 1 + K_{MX}[M^{2+}]$.

The equilibrium relation between free ion concentrations in the membrane and solution for an MA_2 salt, analogous to Eq. (5), results in the following expression for the free anions

$$[A^-] = 2\frac{(S_0 C_S)^{3/2}}{[M^{2+}]^{1/2}}, \tag{10}$$

which is substituted to Eq. (9) and solved to yield $[M^{2+}]$ and $[A^-]$. The total concentration of mobile ions M^{2+} and A^- in the membrane are found as follow

$$C_M^m = X\frac{K_{MX}[M^{2+}]}{1 + K_{MX}[M^{2+}]} + [M^{2+}] \tag{11}$$

and

$$C_A^m = [A^-]. \tag{12}$$

As a next-level scenario, we may consider both MX^+ pairs and MAX triplets. Note that MAX triplet is neutral and thus does not contribute any charge; therefore, the electroneutrality Eq. (9) still holds, but Ξ becomes

$$\Xi = 1 + K_{MX}[M^{2+}] + K_{MAX}[M^{2+}][A^-]. \tag{13}$$

Note the last term is of second order in ion concentration and thus may become important at high salt concentrations. Indeed, below, we will see that it may explain the behavior of $CaCl_2$ at the highest analyzed concentrations (>1 M), where the formation of MX^+ species alone is unable to explain the observed trends.

After solving Eq. (9) along with Eqs. (10) and (13), The total concentration of mobile ions M^{2+} and A^- in the membrane are given by

$$C_M^m = X\frac{K_{MX}[M^{2+}] + K_{MAX}[M^{2+}][A^-]}{1 + K_{MX}[M^{2+}] + K_{MAX}[M^{2+}][A^-]} + [M^{2+}] \tag{14}$$

and

$$C_A^m = X\frac{K_{MAX}[M^{2+}][A^-]}{1 + K_{MX}[M^{2+}] + K_{MAX}[M^{2+}][A^-]} + [A^-]. \tag{15}$$

An alternative second-order modification may consider pairing of

free ions as charged MA^+ pairs instead of MAX triplets. The electroneutrality condition then becomes

$$\frac{-1+K_{MX}\left[M^{2+}\right]}{1+K_{MX}\left[M^{2+}\right]}+\frac{2\left[M^{2+}\right]+\left[MA^{+}\right]-\left[A^{-}\right]}{X}=0 \tag{16}$$

where

$$\left[MA^{+}\right]=K_{MA}\left[M^{2+}\right]\left[A^{-}\right] \tag{17}$$

and, after solving Eq. (16) along with Eqs. (10) and (17) for $[M^{2+}]$ and $[A^-]$ the total concentration of mobile ions in the membrane are found as follows,

$$C_M^m=X\frac{K_{MX}\left[M^{2+}\right]}{1+K_{MX}\left[M^{2+}\right]}+K_{MA}\left[M^{2+}\right]\left[A^{-}\right]+\left[M^{2+}\right]; \tag{18}$$

$$C_A^m=K_{MA}\left[M^{2+}\right]\left[A^{-}\right]+\left[A^{-}\right]. \tag{19}$$

2.3. M_2A salts

For M_2A salts of a monovalent cation and divalent anion, such as Na_2SO_4, assuming MX association only, we obtained the following electroneutrality condition

$$-\frac{1}{1+K_{MX}[M^{+}]}+\frac{[M^{+}]-2\left[A^{2-}\right]}{X}=0 \tag{20}$$

where $[A^{2-}]$ is given by equilibrium with solution as

$$\left[A^{2-}\right]=4\frac{(S_0C_S)^3}{[M^{+}]^2}. \tag{21}$$

When free MA^- pairs are considered as well, Eq. (20) is replaced with

$$-\frac{1}{1+K_{MX}[M^{+}]}+\frac{[M^{+}]-2\left[A^{2-}\right]-[MA^{-}]}{X}=0, \tag{22}$$

with $[MA^-]$ given by

$$[MA^{-}]=K_{MA}[M^{+}]\left[A^{2-}\right]. \tag{23}$$

The total ion concentrations in the membrane are obtained after finding $[M^+]$ and $[A^{2-}]$ by combining and solving these relations, similar to other salts, as follows

$$C_M^m=X\frac{K_{MX}\left[M^{2+}\right]}{1+K_{MX}\left[M^{2+}\right]}+K_{MA}[M^{+}]\left[A^{2-}\right]+[M^{+}]; \tag{24}$$

$$C_A^m=K_{MA}[M^{+}]\left[A^{2-}\right]+\left[A^{2-}\right]. \tag{25}$$

3. Methods

The experimental data, including the uptake of cations and anions in Nafion 117 membranes for NaCl, $MgCl_2$, and Na_2SO_4 single salt solutions, were digitized from Sujanani et al. [24] and for $CaCl_2$ in a CR61 membrane from Galizia et al. [25]. The model was fitted to the experimentally measured concentrations of cations and anions in the membrane. The experimental data, including uptake of cations and anions in Nafion 117 membranes for NaCl, $MgCl_2$, and Na_2SO_4 single salt solutions, were digitized from Sujanani et al. [24] and for $CaCl_2$ in a CR61 membrane from Galizia et al. [25]. The fits were compared with Manning's counterion condensation model, computed as described in the above references.

All the model relations were implemented and fitted to experimental data using Python. The fitted parameters include the membrane fixed charge density X, appropriate equilibrium association constants K's, and salt injection coefficients S_0. Since the parameter space was large, especially the range of *a priori* unknown K's and S_0, the model was solved using a genetic global optimization algorithm included in the Genetic algorithm Python library.

4. Results

Sujanani et al. and Galizia et al. [24,25] reported experimental data for salts of different types and well-known benchmark membranes CR61 and Nafion 117. The ion partitioning data in Nafion span the reasonably large range of external salt concentration 0.01 M–1.0 M, and the results for $CaCl_2$ in CR61 are further extended up to 6 M $CaCl_2$; therefore, they provide a sound basis for modeling. All parameter fitted to corresponding models for all four salts are presented and discussed in the following sections 4.1 to 4.4 and are summarized in Table 1.

4.1. NaCl uptake in Nafion

Fig. 1 compares the results for NaCl uptake in Nafion 117 with the fits to the present model and to the Manning model, as reported by Sujanani et al. [24]. The concentrations shown are per water volume inside the polymer rather than per total membrane volume, which is justified given Nafion has a microphase-separated morphology, with water and ions sharply segregated from the Teflon-like matrix within ionic clusters of a characteristic size of a few nanometers [28–31]. Overall, both models show a similar agreement. Notably, while Sujanani et al. determined the membrane fixed charge density $X = 3.96 \pm 0.1$ M experimentally from sorption experiments with 0.01 M NaCl, the present fitting procedure yielded for NaCl solutions a slightly larger value $X =$ 4.2 M, which should be reasonable, given inherent uncertainties of measured ion uptake, water content, effects of salt type, and variability of the samples stemming from thermal, mechanical and pretreatment history [32].

4.2. $MgCl_2$ uptake in Nafion

Fig. 2 shows the measured $MgCl_2$ uptake in Nafion 117, along with fits to the present association model including MX^+ pairs only, as well as the fits to the Manning model, as reported by Sujanani et al. [24]. Both model fits are commensurate, but the present model deviates more significantly for low concentrations <0.1 M.

We note that at low solution concentrations, the *total* molar content of Mg^{2+} within the membrane approaches half the fixed charge X and becomes virtually independent of the external salt concentration. This suggests that the association-dissociation equilibrium between the MX^+, M^{2+}, and X^- species within the membrane is negligibly affected by Cl^- anions whose content is 2-3 orders smaller. Since the total fixed charge content is constant, the concentration $[M^{2+}]$ becomes about constant in the dilute regime, and then $2[M^{2+}]$ plays the role of an effective fixed charge of the membrane, replacing a genuine constant fixed charge assumed in the Donnan model. As a result, as follows from Eq. (10), the logarithmic slope of the co-ion concentration in the membrane $[A^-]$ versus solution concentration C_s approaches the ideal value 3/2 for the Donnan equilibrium of a dilute MA_2 salt with a charged membrane. This is what is expected at the lowest solution concentration for both the present and Manning models as well. For the same reason, the results in Fig. 1 for NaCl show that the ideal slope of 2 for MA salts (cf. Eq. (5)) is closely approached by both models as the concentration drops. Similar

Table 1
Fitted model parameters for data in Figs. 1 to 4.

Salt/membrane	S_0	K_{MX}, [M^{-1}]	K_{MA}, [M^{-1}]	X [M]
NaCl/Nafion	0.4	4.6×10^2	———	4.2
Na_2SO_4/Nafion	0.02	5.8×10^4	7.9×10^3	4.0
$MgCl_2$/Nafion	0.006	3.4×10^6	———	3.7
$CaCl_2$/CR61	0.006	6.1×10^6	1.7×10^5	2.8

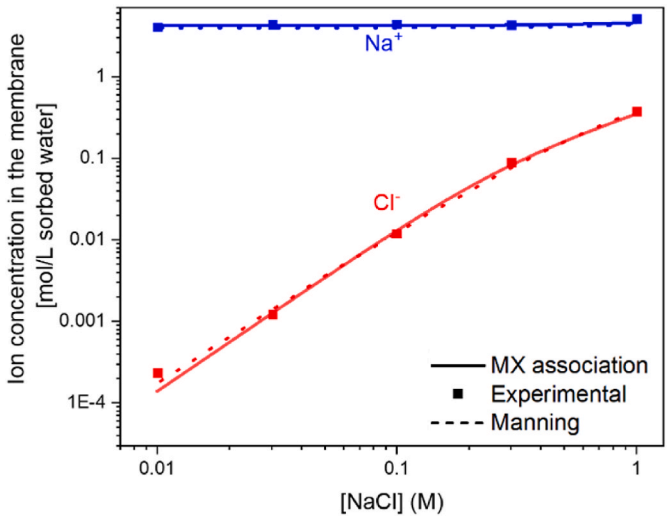

Fig. 1. Concentrations of chloride and sodium ions in the water phase within Nafion vs. sodium chloride concentration in the external solution. Symbols are experimental data from Sujanani et al. [24], solid lines represent fit to the present model, and dotted lines are fit to the Manning model. Fitted parameters values for the present model are $S_0 = 0.4$, $K_{MX} = 4.6\times10^2$ M^{-1}, and X =4.2 M.

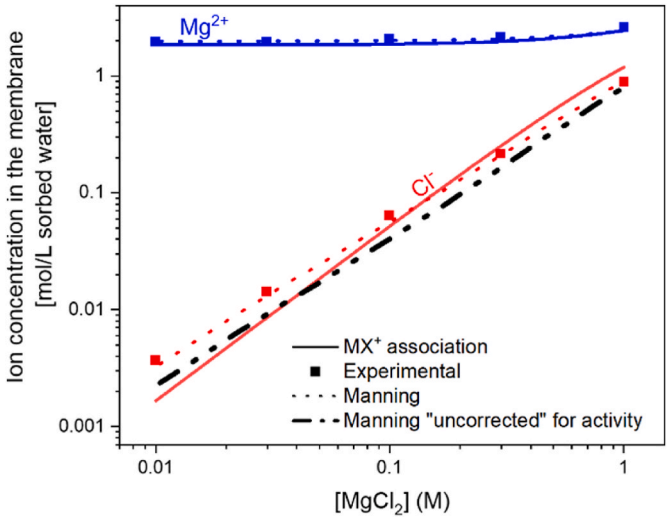

Fig. 2. Concentrations of chloride and magnesium ions in the water phase within Nafion vs. magnesium chloride concentration in the external solution. Symbols are experimental data from Sujanani et al. [24], solid lines represent fit to the present model, and dotted lines are fit to the Manning model. Fitted parameters values for the present model are $S_0 = 0.006$, $K_{MX} = 3.4\times10^6$ M^{-1}, and X = 3.7 M.

to NaCl, it is also observed in the present fit for $MgCl_2$ in Fig. 2; however, the Manning fit shows a slightly lower slope due to the small correction of the Debye-Hückel type for ion-ion interactions, which makes the intra-membrane activity coefficient progressively smaller as the salt concentration increases. This correction is rigidly related to the same parameter that controls the counterion condensation in the Manning model; however, it would be an independent correction in the present model, with more parameters required. In this first analysis, we deem it not critical and therefore examine the relative importance of this correction simply by removing it from the Manning fit rather than adding it to the present model (see Eqs. S1 and S2 and the accompanying discussion in section S1 of the SM). The result is shown in Fig. 2 as the dashed-dotted line and, indeed, nearly eliminates the difference between the two fits. In any case, this correction is small and insignificant here, given the limited amount of available experimental data and possibly, other uncertainties.

Figs. 1 and 2 and Table 1 also show a large difference between fitted S_0 and K_{MX} values for NaCl and $CaCl_2$; thus, S_0 is significantly smaller, and K_{MX} is much larger for $CaCl_2$. This is well expected, given the double charge of Ca^{2+}, resulting in stronger dielectric exclusion and, on the other hand, stronger binding to fixed charges, compared with Na^+.

4.3. Na_2SO_4 uptake in Nafion

Fig. 3 shows fits for Na_2SO_4 uptake in Nafion 117. While the present model yields a reasonable fit, the Manning fit significantly deviates, as noted by Sujanani et al. However, for a fair comparison, we stress that Sujanani et al. employed the same Bjerrum length for the shown Manning fit as for the above two salts rather than an independent fit to adjust the Bjerrum length. The observed deviation of the Manning model may then primarily reflect issues specific to Na_2SO_4 rather than to the Manning model if its parameters were allowed to be salt-specific.

In this particular case, for the monovalent sodium interaction with the fixed sulfonate charges, we expect a relatively weak electrostatic attraction, similar to NaCl. This is well reflected in the magnitude of the fitted association constants, K_{MX}. For the Mg-sulfonate pair, K_{MX} is 3.4×10^6 M^{-1}, which means that, for X ~4 M, the vast majority of fixed charges is associated. For NaCl and Na_2SO_4 uptake, the fitted K_{MX} values for the Na-sulfonate pair are several orders of magnitude lower, i.e., a significant proportion of fixed charges is dissociated. However, even if not as much as for $MgCl_2$, the fitted K_{MX} values for NaCl and Na_2SO_4, 4.6×10^2 and 5.8×10^4 M^{-1}, respectively, differ significantly as well, despite the fact that they represent the same NaX pair. We presume that it may be related to numerical redundancy, making parameters interdependent, as discussed in Section 4.5.

4.4. $CaCl_2$ uptake in CR61

Like $MgCl_2$, $CaCl_2$ is an MA_2-type salt. Fig. 4 shows its uptake in CR61 up to 6 M reported by Galizia et al. [25]. A wider studied range, compared with $MgCl_2$ in Nafion (Section 4.2), enables better analysis of the high-salt regime, where pairing should be greatly enhanced. Fig. 4a indicates that both the regular Manning and the present model, including MX^+ pairs only, clearly deviate from experimental data above

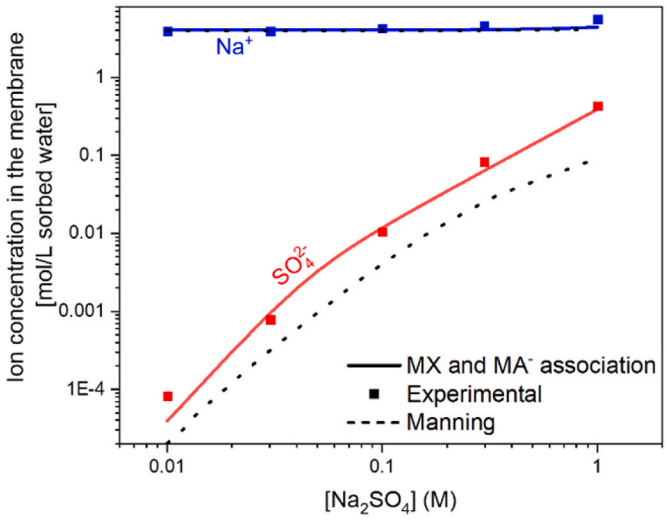

Fig. 3. Concentrations of sulfate and sodium in the water phase within Nafion vs. sodium sulfate concentration in the external solution. Symbols are experimental data from Sujanani et al. [24], solid lines represent fit to the present model, and dotted lines are fit to the Manning model. Fitted parameters values for the present model are $S_0 = 0.02$, $K_{MX} = 5.8\times10^4$ M^{-1}, $K_{MA} = 7.9\times10^4$ M^{-1} and X =4.03 M.

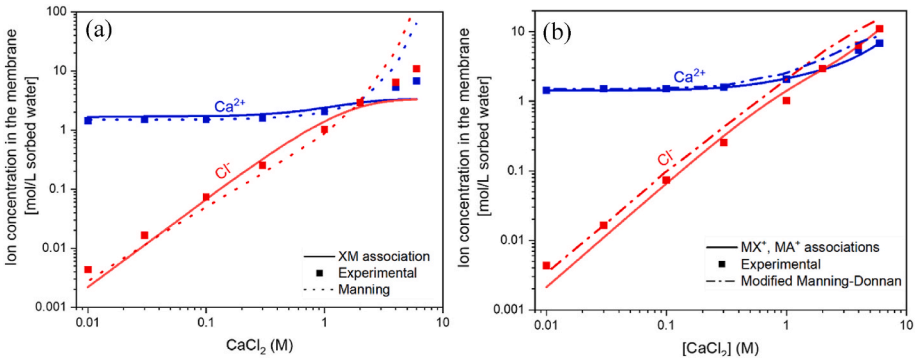

Fig. 4. Concentrations of calcium and chloride ions in the water phase within CR61 vs. calcium chloride concentration in the external solution. Symbols are experimental data from Galizia et al. [25]. Solid lines represent fits to the present model and dotted lines are fits to the Manning model. In panel (a), the fits are to the present model including MX pairs only and to the regular Manning model; in panel (b), the fits are to the present model, including both MX and MA pairs and to the modified Manning-Donnan model of Galicia et al. [25]. Fitted parameters values for the present model in panel (b) are S_0=0.006, K_{MX} =6.1 × 10^6 M^{-1}, K_{MA} =1.7 × 10^5 M^{-1}, and X = 2.80 M.

1 M (See also Fig. S1 and the accompanying discussion in section S2 of Supplementary Material). For this region, improved fits are shown in Fig. 4b. One proposed by Galizia et al. modifies the Manning-model using an empirical correction that allows a high ion activity with an ion activity coefficient greater than one [25]. The present model produces an improved fit by allowing the formation of both MX^+ and charged free-ion pairs MA^+, similar to the case of Na_2SO_4. Indeed, the existence of $CaCl^+$ ion pairs was reported even in pure water [33,34] therefore it is well expected in the lower dielectric environment within the membrane. Note that an activity coefficient smaller than one, i.e., higher salt concentration in the membrane compared with solution in the most concentrated range in Fig. 4, is a likely indication of ion association that is known to occur at high $CaCl_2$ concentrations in solution, >2 M [35,36], and justifies the need to include $CaCl^+$ pairs here as a natural extension of the present model. We also note that fitted salt injection coefficients S_0 are of the same order of magnitude for $CaCl_2$ and Na_2SO_4, as expected for MA_2 and M_2A salts (see Figs. 3 and 4).

4.5. Numerical redundancy of the model parameters

The above models for different salts contain 3 or 4 parameters that are supposed to be mutually independent. However, deriving the full set requires that the range of salt concentration allow transition between several regimes of ion uptake, where parameters combine differently, which is unfortunately not the case. Specifically, we observe that, except for the highest concentration of $CaCl_2$ in CR61, the measured amount of co-ions remains fairly insignificant relative to counterions in the entire range. In this case, arbitrary variation of some of them is effectively offset by variation of other parameters, i.e., there is a *numerical redundancy* thus not all parameters may be fitted with confidence.

This may be illustrated using as an example the relations for uptake of NaCl. The much lower content of anions in the membrane compared with cations (Fig. 1) and, on the other hand, high cation content that may strongly promote the formation of MX pairs makes it likely that Eq. (4), electroneutrality condition, is simplified to

$$-\frac{1}{K_{MX}[M^+]}+\frac{[M^+]}{X}\approx 0. \tag{26}$$

thereby Eqs. (26) and (8) yield

$$[M^+]\approx\left(\frac{X}{K_{MX}}\right)^{1/2},[A^-]\approx\left(\frac{K_{MX}}{X}\right)^{1/2}(S_0C_S)^2,C_A^m=[A^-]\approx\left(\frac{K_{MX}}{X}\right)^{1/2}(S_0C_S)^2. \tag{27}$$

X is relatively rigidly fixed by the plateau of measured $C_M^m = X + C_A^m \approx X$, in particular, at the lower salt concentrations, but the last relation in Eq. 27 identifies $S_0^2(K_{MX}/X)^{1/2}$ as a lumped parameter or *combination* that dictates the dependence of the measured anion content C_A^m on C_s in the lower concentration range.

Under an alternative assumption that the MX association is insignificant, we would have, $[M^+]\approx X, [A^-]\approx (S_0C_S)^2/X$, hence

$$C_A^m\approx (S_0C_S)^2/X. \tag{28}$$

and the appropriate lumped parameter is $S_0^2X^{-1}$. Both Eqs. (27) and (28) predict that that C_A^m is proportional to C_S squared, which is observed in Fig. 1 in nearly entire range, as discussed in Section 4.2. This dependence confirms that $[A^-]$ is far below $[M^+]$ and not just smaller than X, but only the prefactor F_2 that multiplies C_S^2 may be determined with confidence, while the specific values of S_0 and K_{XM}, and even whether F_2 is defined by eq. 27 or 28, are uncertain.

In the case of Na_2SO_4 as another example, we observe the counterion is the same as in the case of NaCl and the anions A^{2-} are far fewer than cations in the membrane (Fig. 3) but, likely, they are mainly present as MA^- pairs. If these pairs are still fewer than free M^+ ions, i.e., $[MA^-] << [M^+]$, Eqs. (21) and (23) yield

$$C_A^m\approx[MA^-]\propto C_S^3, \tag{29}$$

where the prefactor F_3 is either $4K_{MA}S_0^3(K_{MX}/X)^{1/2}$ in the case of strong MX association, when $[M^+]\approx(X/K_{MX})^{1/2}$ or $4K_{MA}S_0^3X^{-1}$ in the case MX association is negligible thus $[M^+]\approx X$. The cubic dependence $C_A^m\propto C_S^3$ that seems to be observed in low concentration range in Fig. 3 cannot differentiate between these scenarios and, in any case, would not allow definitive fitting of all parameters.

However, Fig. 3 also indicates that the cubic regime does not cover the entire concentration range and there is a transition in the middle range to a dependence with a smaller exponent, close to 3/2. This is successfully fitted only using a sufficiently large value of K_{MA}, i.e., very strong MA association. As a result, $[MA^-]$ eventually exceeds the free cation concentration $[M^+]\approx(X/K_{MX})^{1/2}$ released by fixed charge dissociation thus the M^+ inherently present in the membrane cannot balance the negative charge of invading MA^- pairs. Instead, it has to be balanced by invasion of M^+ ions from solution (see also computed speciation of ions in Section S3 and Fig. S2 in Supplementary Material). In this regime, electroneutrality condition is approximated as

$$[M^+]\approx[MA^-]=K_{MA}[M^+][A^{2-}], \tag{30}$$

whence $[A^{2-}]\approx 1/K_{MA}$ and, using Eqs. (21) and (23), we obtain

$$C_A^m\approx[MA^-]\approx 2K_{MA}^{1/2}(S_0C_S)^{3/2}. \tag{31}$$

This dependence $C_A^m \propto C_S^{3/2}$ is indeed close to the one observed at the higher concentrations in Fig. 3 and the relevant combination defining this dependence is $2K_{MA}^{1/2}S_0^{3/2}$.

We note at this point that the observed $C_S^{3/2}$ dependence for Na_2SO_4 rules out the scenario of negligible MX association with $[M^+] \approx X$ considered above, since this would also rule out Eq. (30), in which case the cubic trend would continue for Na_2SO_4 as long as there are much fewer anions than cations in the membrane. Turning back to the previous case of NaCl, this rules out the scenario given by eq. (28), therefore the prefactor defining the C_S^2 dependence of anion uptake must be $F_2 = S_0^2(K_{MX}/X)^{1/2}$.

Ultimately, for Na_2SO_4, the presence of two regimes defines three quantities, $C_M^m \approx X$, the prefactor $F_{3/2} = 2K_{MA}^{1/2}S_0^{3/2}$ of the 3/2-exponent dependence of C_A^m in the upper range (Eq. (31)), and the prefactor $F_3 = 4K_{MA}S_0^3(K_{MX}/X)^{1/2} = F_{3/2}^2(K_{MX}/X)^{1/2}$ of the cubic dependence in lower range (Eq. (29)). This reduces numerical redundancy but still cannot eliminate it, thus all four parameters cannot be defined with certainty from these three quantities. Similarly, for NaCl, the corresponding quantities are X and $F_2 = S_0^2(K_{MX}/X)^{1/2}$, which cannot determine with certainty the three defined parameters. This uncertainty is a likely reason for discrepancy between the fitted K_{XM} values for NaCl and Na_2SO_4. Specifically, we note that fitted X, F_3, and $F_{3/2}$ fully define K_{XM} for Na_2SO_4, therefore its fitted value may be treated with more confidence, but X and F_2 only fix the combination $S_0^2K_{MX}^{1/2}$ for NaCl. Therefore, the fitted values of S_0 and K_{MX} for NaCl listed in Table 1 are less certain, as well as the values of S_0 and K_{MA} combining in $F_{3/2}$ for Na_2SO_4.

Nevertheless, if observable, the transition to the highest-concentration regime when salt uptake approaches fixed charge may ease the redundancy. Unfortunately, this transition is barely present in Figs. 1 to 3 and keeps the significant uncertainty of S_0 and K's in place. Its small effect on fits may explain why fitted S_0 for Na_2SO_4 is smaller than for NaCl, as expected due to the stronger exclusion of sulfate compared with chloride, but the disparate K_{MX} values emphasize the remaining uncertainties apparently related to numerical redundance. On the other hand, the highly concentrated regime is well resolved in Fig. 4 for $CaCl_2$ in CR61 and fitted parameters may be viewed with somewhat more confidence. Thus, the K_{MX} values for calcium in CR61 and for magnesium in Nafion are expectedly commensurate and larger than for NaCl, and respective S_0 values are correspondingly smaller.

In summary, the present data cover a limited concentration range for each salt and may not include all possible regimes covered by the model, namely, full or partial dissociation of fixed charged and free ions as well as invading salt being negligible or surpassing the fixed charge. Therefore, certain regimes of the models dominate throughout, while the others do not show up. The is seen more explicitly in the speciation of ions to different free and associated forms according to the best fits, presented in more detail in section S3 and in Fig. S2 in Supplementary Material. Without all regimes present in experimental results or additional data quantifying ion association, e.g., electrical measurements, it may be difficult to ascertain in each case whether the fitted parameters reflect their true values or lump some other effects as well.

4.6. Manning model versus presented model and physical redundancy

The defining parameter for Manning's counterion condensation theory is the dimensionless charge density, ξ_M, for which Sujanani et al. used the value determined by Kamcev et al. for HCl sorption in Nafion 117 [37]. Since this $\xi_M = 0.31$ exceeds the critical values, $\xi_c = |z_i z_p|^{-1}$, for all analyzed salts in Nafion, NaCl, $MgCl_2$, and Na_2SO_4, the model of Sujanani et al. predicts that a commensurate fraction of both counterions, Mg^{2+} and Na^+, is condensed. While a strong association should indeed be a sound assumption for the divalent Mg^{2+}, it is less likely that monovalent Na^+ will be dissociated to a similar degree, given their different charge and also much different charge densities, respectively, 120 and 24 C mm^{-3} [39]. The several orders of magnitude difference in fitted association constants K_{MX} of the two counterions seem more reasonable than the fairly small factor 2 separating ξ_c of the two ions in the Manning model. The species distribution is quantified and shown in Fig. S2, which further illustrates the influence of association constants. Münchinger and Kreuer compared Manning's counterion condensation theory with their experimental data on competitive Cs^+/Li^+ sorption in Nafion 117 and spin relaxation measured for these ions by NMR [27]. From NMR measurements, they estimated the association constant for Cs-sulfonate pairs to be $K_{CsX} = 4$ M^{-1}. This value is substantially lower than our fitted $K_{NaX} = 4\times10^2$ M^{-1}, while Münchinger and Kreuer argued that, within the alkaline metals, Na^+ is smaller, harder, and less polarizable than Cs^+, which would lead to a stronger interaction, thus K_{CsX} should be smaller than K_{NaX} [27]. The difference might, once again, be due to the numerical redundancy and/or K_{NaX} also lumping ion-ion interactions.

We conclude the discussion by noting that apart from numerical redundancy discussed in the last section, there may also be physical redundancy, resulting in inter-dependence of parameters on the physical grounds. Specifically, the relative permittivity of the membrane is supposed to affect both ion association and free ion uptake in a correlated manner [21], as it does in the Manning model; however, the association constants K_{MX} and K_{MA} and salt injection coefficient S_0 are treated as independent in our model. Some decoupling between the two types of parameters is possible if the microenvironment within the membrane is not homogeneous; thus, ion pairs, especially of MX type, and free ions may face a somewhat different microenvironment and solvation. This is likely within Nafion, known to have microphase-separated morphology, where sulfonic groups line the boundary of a few nanometers large domains containing water and free ions and may be more strongly affected by adjacent hydrophobic matrix than co- and counterions within such domains. As discussed in the opening of Section 2, ion-ion interactions may also affect differently and further decouple these parameters. Additional factors, possibly contributing to the decoupling of these parameters, were discussed in Ref. [21]. However, the present results seem insufficient to claim conclusively that solvation and association are fully decoupled and thus S_0 and K's may be treated as independent. This presents an open question for future research.

5. Conclusion

The ion association theory in the formulation going back to Bjerrum provides a sound physicochemical basis for understanding ion exchange membranes that is distinctly different and potentially better addresses ion-specificity than the Manning condensation model. As such, it can readily include various types of associates that involve both fixed and mobile ions, subject to experimentally observed trends, and better match measured results. These features seem most advantageous for modeling the ion uptake behavior for M_2A- and MA_2-type electrolytes, especially at the largest salt concentration, where the association is significant. This was demonstrated by fitting the present model to the available experimental data for the uptake of several salts, including Na_2SO_4, $MgCl_2$, $CaCl_2$, and NaCl, in two cation-exchange resins. The fitted values of the defined parameters with a clear physical meaning are subject to uncertainties certain due to limited observed range and some regimes being absent or insufficiently resolved. Yet, the found values appear to be consistent with trends expected for partitioning and speciation of different ions based on their charge and with other data. Overall, the present model consistently incorporates ion association and thus amends the previously used physical picture, based on the Donnan model or its modification. It offers a useful framework for modeling, understanding, and predicting ion uptake in ion-exchange and related materials.

Author statement

Yaeli S. Oren: Methodology, Analysis, Investigation and Writing – Original Draft.

Oded Nir: Writing – Review & Editing, Supervision.

Viatcheslav Freger: Conceptualization, Methodology, Writing – Original Draft, Review & Editing, Supervision.

All authors have read and agreed to the published version of the manuscript.

Declaration of competing interest

The authors declare the following financial interests/personal relationships which may be considered as potential competing interests: Oded Nir reports financial support was provided by Binational Science Foundation. Viatcheslav Freger reports financial support was provided by Horizon Europe.

Data availability

Data will be made available on request.

Acknowledgements

This work was financially supported by the US National Science Foundation (NSF) and US–Israel Binational Science Foundation (BSF) under award no. CBET-2110138. V.F. acknowledges support from the European Union's Horizon 2020 research and innovation programme under grant agreement No 862100 (NewSkin). Y.O. would like to thank the Kreitman School of Advanced Graduate Studies for support through the Hightech, Biotech, and Chemotech scholarship program.

Appendix A. Supplementary data

Supplementary data to this article can be found online at https://doi.org/10.1016/j.memsci.2023.122202.

References

[1] S. Jiang, H. Sun, H. Wang, B.P. Ladewig, Z. Yao, A comprehensive review on the synthesis and applications of ion exchange membranes, Chemosphere 282 (2021), 130817, https://doi.org/10.1016/j.chemosphere.2021.130817.

[2] J. Ran, L. Wu, Y. He, Z. Yang, Y. Wang, C. Jiang, L. Ge, E. Bakangura, T. Xu, Ion exchange membranes: new developments and applications, J. Membr. Sci. 522 (2017) 267–291, https://doi.org/10.1016/j.memsci.2016.09.033.

[3] T. Xu, C. Huang, Electrodialysis-based separation technologies: a critical review, AIChE J. 54 (2008) 3147–3159, https://doi.org/10.1002/aic.11643.

[4] N.Y. Yip, D.A. Vermaas, K. Nijmeijer, M. Elimelech, Thermodynamic, energy efficiency, and power density analysis of reverse electrodialysis power generation with natural salinity gradients, Environ. Sci. Technol. 48 (2014) 4925–4936, https://doi.org/10.1021/es5005413.

[5] S. Maurya, S.-H. Shin, Y. Kim, S.-H. Moon, A review on recent developments of anion exchange membranes for fuel cells and redox flow batteries, RSC Adv. 5 (2015) 37206–37230, https://doi.org/10.1039/C5RA04741B.

[6] E. te Brinke, D.M. Reurink, I. Achterhuis, J. de Grooth, W.M. de Vos, Asymmetric polyelectrolyte multilayer membranes with ultrathin separation layers for highly efficient micropollutant removal, Appl. Mater. Today 18 (2020), 100471, https://doi.org/10.1016/j.apmt.2019.100471.

[7] Y. Yang, Y. Li, K. Goh, C.H. Tan, R. Wang, Dopamine-intercalated polyelectrolyte multilayered nanofiltration membranes: toward high permselectivity and ion-ion selectivity, J. Membr. Sci. 648 (2022), 120337, https://doi.org/10.1016/j.memsci.2022.120337.

[8] C. Huang, T. Xu, Electrodialysis with bipolar membranes for sustainable development, Environ. Sci. Technol. 40 (2006) 5233–5243, https://doi.org/10.1021/es060039p.

[9] M. Zelner, M. Stolov, T. Tendler, P. Jahn, M. Ulbricht, V. Freger, Elucidating ion transport mechanism in polyelectrolyte-complex membranes, J. Membr. Sci. 658 (2022), 120757, https://doi.org/10.1016/j.memsci.2022.120757.

[10] S.M. Hosseini, M.M.B. Usefi, M. Habibi, F. Parvizian, B. Van der Bruggen, A. Ahmadi, M. Nemati, Fabrication of mixed matrix anion exchange membrane decorated with polyaniline nanoparticles to chloride and sulfate ions removal from water, Ionics 25 (2019) 6135–6145, https://doi.org/10.1007/s11581-019-03151-w.

[11] L. Li, N. Akhtar Qaisrani, L. Ma, L. Bai, A. Zhang, G. He, F. Zhang, Mixed matrix anion exchange membrane containing covalent organic frameworks: ultra-low IEC but medium conductivity, Appl. Surf. Sci. 560 (2021), 149909, https://doi.org/10.1016/j.apsusc.2021.149909.

[12] T. Luo, S. Abdu, M. Wessling, Selectivity of ion exchange membranes: a review, J. Membr. Sci. 555 (2018) 429–454, https://doi.org/10.1016/j.memsci.2018.03.051.

[13] H.B. Park, J. Kamcev, L.M. Robeson, M. Elimelech, B.D. Freeman, Maximizing the right stuff: the trade-off between membrane permeability and selectivity, Science 356 (2017), eaab0530, https://doi.org/10.1126/science.aab0530.

[14] V.I. Zabolotsky, V.V. Nikonenko, Effect of structural membrane inhomogeneity on transport properties, J. Membr. Sci. 79 (1993) 181–198, https://doi.org/10.1016/0376-7388(93)85115-D.

[15] Heterogeneity of Ion-Exchange Membranes: The Effects of Membrane Heterogeneity on Transport Properties | Elsevier Enhanced Reader, (n.d.). https://doi.org/10.1006/jcis.2001.7710.

[16] Y. Mizutani, M. Nishimura, Studies on ion-exchange membranes. XXXII. Heterogeneity in ion-exchange membranes, J. Appl. Polym. Sci. 14 (1970) 1847–1856, https://doi.org/10.1002/app.1970.070140718.

[17] J. Kamcev, D.R. Paul, G.S. Manning, B.D. Freeman, Predicting salt permeability coefficients in highly swollen, highly charged ion exchange membranes, ACS Appl. Mater. Interfaces 9 (2017) 4044–4056, https://doi.org/10.1021/acsami.6b14902.

[18] D. Kitto, J. Kamcev, Manning condensation in ion exchange membranes: a review on ion partitioning and diffusion models, J. Polym. Sci. 60 (2022) 2929–2973, https://doi.org/10.1002/pol.20210810.

[19] Y. Yu, N. Yan, B.D. Freeman, C.-C. Chen, Mobile ion partitioning in ion exchange membranes immersed in saline solutions, J. Membr. Sci. 620 (2021), 118760, https://doi.org/10.1016/j.memsci.2020.118760.

[20] N. Yan, D.R. Paul, B.D. Freeman, Water and ion sorption in a series of cross-linked AMPS/PEGDA hydrogel membranes, Polymer 146 (2018) 196–208, https://doi.org/10.1016/j.polymer.2018.05.021.

[21] V. Freger, Ion partitioning and permeation in charged low-T* membranes, Adv. Colloid Interface Sci. 277 (2020), 102107, https://doi.org/10.1016/j.cis.2020.102107.

[22] V. Neklyudov, V. Freger, Putting together the puzzle of ion transfer in single-digit carbon nanotubes: mean-field meets ab initio, Nanoscale 14 (2022) 8677–8690, https://doi.org/10.1039/D1NR08073C.

[23] V. Freger, Selectivity and polarization in water channel membranes: lessons learned from polymeric membranes and CNTs, Faraday Discuss 209 (2018) 371–388, https://doi.org/10.1039/C8FD00054A.

[24] R. Sujanani, L.E. Katz, D.R. Paul, B.D. Freeman, Aqueous ion partitioning in Nafion: applicability of Manning's counter-ion condensation theory, J. Membr. Sci. 638 (2021), 119687, https://doi.org/10.1016/j.memsci.2021.119687.

[25] M. Galizia, G.S. Manning, D.R. Paul, B.D. Freeman, Ion partitioning between brines and ion exchange polymers, Polymer 165 (2019) 91–100, https://doi.org/10.1016/j.polymer.2019.01.026.

[26] K.M. Beers, D.T. Hallinan Jr., X. Wang, J.A. Pople, N.P. Balsara, Counterion condensation in nafion, Macromolecules 44 (2011) 8866–8870, https://doi.org/10.1021/ma2015084.

[27] A. Münchinger, K.-D. Kreuer, Selective ion transport through hydrated cation and anion exchange membranes I. The effect of specific interactions, J. Membr. Sci. 592 (2019), 117372, https://doi.org/10.1016/j.memsci.2019.117372.

[28] A. Yaroshchuk, M.L. Bruening, E. Zholkovskiy, Modelling nanofiltration of electrolyte solutions, Adv. Colloid Interface Sci. 268 (2019) 39–63, https://doi.org/10.1016/j.cis.2019.03.004.

[29] H.-G. Haubold, Th Vad, H. Jungbluth, P. Hiller, Nano structure of NAFION: a SAXS study, Electrochim. Acta 46 (2001) 1559–1563, https://doi.org/10.1016/S0013-4686(00)00753-2.

[30] Z. Liang, W. Chen, J. Liu, S. Wang, Z. Zhou, W. Li, G. Sun, Q. Xin, FT-IR study of the microstructure of Nafion® membrane, J. Membr. Sci. 233 (2004) 39–44, https://doi.org/10.1016/j.memsci.2003.12.008.

[31] A.-L. Rollet, O. Diat, G. Gebel, A new insight into nafion structure, J. Phys. Chem. B 106 (2002) 3033–3036, https://doi.org/10.1021/jp020245t.

[32] W. Xie, G.M. Geise, B.D. Freeman, C.H. Lee, J.E. McGrath, Influence of processing history on water and salt transport properties of disulfonated polysulfone random copolymers, Polymer 53 (2012) 1581–1592, https://doi.org/10.1016/j.polymer.2012.01.046.

[33] S. Friesen, G. Hefter, R. Buchner, Cation hydration and ion pairing in aqueous solutions of MgCl2 and CaCl2, J. Phys. Chem. B 123 (2019) 891–900, https://doi.org/10.1021/acs.jpcb.8b11131.

[34] Y. Marcus, On the activity coefficients of charge-symmetrical ion pairs, J. Mol. Liq. 123 (2006) 8–13, https://doi.org/10.1016/j.molliq.2005.04.008.

[35] J.A. Rard, S.L. Clegg, Critical evaluation of the thermodynamic properties of aqueous calcium chloride. 1. Osmotic and activity coefficients of 0−10.77 mol·kg^{-1} aqueous calcium chloride solutions at 298.15 K and correlation with extended pitzer ion-interaction models, J. Chem. Eng. Data 42 (1997) 819–849, https://doi.org/10.1021/je9700582.

[36] J. Kamcev, M. Galizia, F.M. Benedetti, E.-S. Jang, D.R. Paul, B.D. Freeman, G. S. Manning, Partitioning of mobile ions between ion exchange polymers and aqueous salt solutions: importance of counter-ion condensation, Phys. Chem. Chem. Phys. 18 (2016) 6021–6031, https://doi.org/10.1039/C5CP06747B.

[37] G. Rayner-Canham, T. Overton, Descriptive Inorganic Chemistry, sixth ed., W. H. Freeman, New York, 2013.